Laser and Particle Beams (2011), *29*, 45–54.

doi:10.1017/S0263034610000741

Analytical and numerical investigation of pulse-shape effect on the interaction of an ultrashort, intense, few-cycle laser pulse with a thin plasma layer

HARISH MALAV,[1] K. P. MAHESHWARI,[1] AND Y. CHOYAL[2]

[1]DST-Project, Vardhaman Mahaveer Open University, Kota, India
[2]School of Physics, Devi Ahilya University, Indore, India

(RECEIVED 17 August 2010; ACCEPTED 26 October 2010)

Abstract

Dependence of quasistatic Wakefield and high harmonic generation on the pulse-shape of an ultrashort, intense, few-cycle laser in the reflected radiation from a thin dense plasma layer is investigated. The pulse envelopes considered are Gaussian, Lorentzian, and hyperbolic secant having identical full width at half maximum of intensity. The reflected radiation from the strongly driven surface plasma layer embodies a quasistatic Wakefield, which exists after the main pulse is passed over. A phase modulation is also experienced by the laser light upon reflection from plasma surface motion. As a result harmonics of center carrier frequency of the laser-pulse are generated in the reflected signal. Intensity of the laser harmonics and magnitude of the Wakefield in the reflected radiation are found to depend on the pulse-shape, number of cycles, carrier envelope phase difference, plasma density, angle of incidence, and intensity of the incident pulse.

Keywords: Carrier envelope phase difference; High-harmonic generation; Short laser pulse interaction with thin plasma layer; Wakefield

1. INTRODUCTION

With the advent of high power lasers, it has become possible to study the interaction of free electrons with high intensity laser pulses. By "high intensity" laser field E_0 of center carrier frequency ω_0, we mean that it satisfies the condition: $a_0 \geq 1$, where $\left(a_0 = \frac{eE_0}{mc\omega_0} \sim 10^{-9}\lambda(\mu\,\mathrm{m})\sqrt{I\left(\frac{W}{cm^2}\right)}\right)$. At these intensities electron quiver velocities are close to the velocity of light and the motion of even free electrons becomes highly nonlinear. The nonlinear laser-plasma interaction gives rise to a variety of phenomena like X-ray generation (Kieffer *et al.*, 1992), γ-ray generation (Norreys *et al.*, 1999) relativistic self-focusing (Sprangle, 1987), high-harmonic generation (Linde, 1999; Nuzzo *et al.*, 2000; Villoresi *et al.*, 2001; Nisoli *et al.*, 2003; Foldes *et al.*, 2003; Bulanov *et al.*, 2003; Baeva *et al.*, 2006; Gupta *et al.*, 2007; Varró, 2007; Ganeev, 2009), electron and proton acceleration (Malka *et al.*, 2002; Zepf *et al.*, 2003; Bingham *et al.*, 2004). When such an intense laser is incident on a thin metal layer, an ultrathin, highly inhomogeneous dense plasma layer is created. The electromagnetic field is almost localized in a narrow region in the vicinity of the boundary, which can be modeled as a thin plasma slab. Laser pulse interaction with a very thin slab of over-dense plasma brings in new features that are not encountered in underdense plasmas (Vshivkov *et al.*, 1998). These effects show up prominently when the incident laser pulse contains only few-cycles.

In the present work, we consider an ultrashort few-cycle laser pulse having central carrier frequency ω_0, wave vector $\vec{k}$, and dimensionless amplitude a_0 ncident on a thin plasma layer. The thickness l of the layer is assumed to be much smaller than the average skin depth of incoming radiation and wavelength of laser. The laser pulse is assumed to be *p*-polarized transverse magnetic (TM) wave. The electron plasma frequency ω_p is greater than ω_0. The plasma density varies from solid to vacuum in a distance less than the wavelength. As a result of the interaction of laser pulse with such highly inhomogeneous plasma, the surface electromagnetic waves on plasma-vacuum interface are generated (Dromey *et al.*, 2007; Bulanov *et al.*, 2007). The character of surface waves depends on the boundary conditions, which must supplement the field equations.

Varró (2007) has shown that in the scattered radiation generated by an ultrashort, intense, few-cycle laser pulse

Address correspondence and reprint requests to: K. P. Maheshwari, DST-Project, Vardhaman Mahaveer Open University, Rawatbhata road, Kota-324010, India. E-mail: k_p_maheshwari@rediffmail.com

impinging on a metal nano-layer, nonoscillatory Wakefield appears with a definite sign. This quasistatic field remains for many more periods of the main pulse. In this paper, we analyze the effect of the pulse-shape on the excitation of the quasistatic Wakefield. We find that the magnitude and sign of this left-over field depends on the pulse-shape, carrier envelope phase (CEP), thickness of the plasma layer, angle of incidence of the laser and gradient of the plasma density. The pulse-shapes considered are Gaussian, Lorentzian, and hyperbolic secant having identical full width at half maximum (FWHM) of intensity. Following Brabec and Krausz (1997, 2000), we have made use of the powerful concept of the envelope for few-cycle laser pulses up to the limit of single cycle.

Generation of high harmonics from a solid target can be understood in terms of coherent wake emission (CWE) (Quéré *et al.*, 2006; Brügge & Pukhov, 2007; Dromey *et al.*, 2009). CWE mechanism is predominant at moderately relativistic intensities ($a_0 \sim 1$) and short, but finite plasma gradient lengths. Because of the density inhomogeneity, the electrostatic oscillations couple back to electromagnetic modes. A transient phase matching between the electromagnetic field and plasma oscillations with a density gradient leads to the emission of harmonics of the incident frequency (Quéré *et al.*, 2006, 2008). Relativistic effects modify the nonlinear processes that are known in the limit of moderate radiation amplitudes. In this paper, we consider the reflection and transmission of an oblique incident electromagnetic few-cycle laser pulse from a highly inhomogeneous plasma layer following the model introduced by Varró (2007). This model includes radiation reaction term resulting in phenomenological damping in the equation of motion of the plasma layer. In the present study, we follow the same model that include the effect of the specific pulse-shape, angle of incidence, CEP of the laser pulse, number of cycles in a pulse on the high harmonic generation.

The paper is organized as follows: In section 2, we analyze the dependence of the quasistatic Wakefield on the pulse-shape of an ultrashort, intense, few cycle laser in the reflected radiation from a thin, dense plasma layer. Dependence of high harmonic generation on the pulse-shape of an ultrashort, intense, few cycle laser in the reflected radiation from a thin, dense plasma layer is given in Section 3. Results and discussion are presented in Section 4. Finally, Section 5 presents our conclusions.

2. DEPENDENCE OF QUASISTATIC WAKEFIELDS ON THE PULSE SHAPE OF AN ULTRASHORT, INTENSE, FEW CYCLE LASER IN THE REFLECTED RADIATION FROM A THIN, DENSE PLASMA LAYER

We consider an ultrashort few-cycle laser pulse with central carrier frequency ω_0, wave vector $\vec{k}$, and dimensionless amplitude $a = eE/mc\omega_0$, impinging on a plasma thin layer, lying between $z = -l/2$ and $z = l/2$, is located at $x = 0$, here e and m denote the charge and rest mass of the electron, respectively. The thickness l of the plasma layer is assumed to be much smaller than the average skin depth of incoming radiation. The wave vector $\vec{k} = (0, k\sin\theta, -k\cos\theta)$ makes an angle θ with the z-axis. The plane of incidence is y–z plane. The laser pulse is assumed to be p-polarized TM wave with electric fields $\vec{E} = (0, E_y, E_z)$ and magnetic field $\vec{B} = (B_x, 0, 0)$. The plasma density N drops to zero over a length much less than laser wavelength. In over-dense plasma the penetration length of the electromagnetic wave, $d_e = c/\omega_p$ is small compared to its wavelength in vacuum λ. Here c is the speed of light in vacuum, and $\omega_p = \sqrt{4\pi Ne^2/m}$ is the plasma frequency. The interaction of the laser with thin plasma layer gives rise to the generation of surface electromagnetic waves on a semi-bounded plasma-vacuum interface. The character of surface waves essentially depends on the boundary conditions, which must supplement the field equations. The dimensionless parameter $k = \omega_p^2 l/2\omega_0 c \equiv \lambda l/4\pi\, d_e^2$, gives a measure of the transparency ($k \ll 1$) or opaqueness ($k \gg 1$) of the plasma layer.

Following Varró (2007), the reflected field $f_1(t')$ from thin plasma layer in the region-1($z > l/2$) can be represented in terms of the y-component of the local velocity $\delta_y'(t') = \left(d\delta_y(t')/dt'\right)$, of the electrons in the plasma layer:

$$f_1(t') = -\frac{m\Gamma}{e}\left[\frac{d\delta_y(t')}{dt'}\right] \tag{1}$$

Where $t' = t - y\sin\theta/c$ is the retarded time, $\Gamma = \left(\omega_p/\omega_0\right)^2 \left(\pi l/\lambda\right)\omega_0$ is the damping parameter.

The local velocity $\delta_y'(t')$ is obtained by solving the following equation of motion for electrons in presence of complete electric field:

$$\frac{d^2\delta_y(t')}{dt'^2} = \cos\theta\left[\frac{e}{m}F(t') - \Gamma\left(\frac{d\delta_y(t')}{dt'}\right)\right] \tag{2}$$

where $F(t)$ represents the field of the incident laser pulse.

We consider various analytic pulse-shapes, $F(t) = A(t)\cos\left(\omega_0 t + \phi\right)$ where $A(t)$ is the envelope of the pulse. The envelopes for a Gaussian, Lorentzian, and hyperbolic secant pulses are taken to be $A_g(t) = F_0 \exp\left[-\left(1.17t/\tau\right)^2\right]$, $A_l(t) = F_0\left[1/1 + \left(1.29t/\tau\right)^2\right]$, and $A_h(t) = F_0 \mathrm{sech}\left(1.76t/\tau\right)$, respectively, where τ is FWHM of pulse intensity and ϕ is carrier envelope phase (Brabec & Krausz, 1997).

Solving Eq. (2), the asymptotic behavior of the local velocity $\left(d\delta_y(t')/dt'\right)$, for different temporal envelopes of the laser pulse, can be expressed as:

$$\left[\frac{d\delta_y(t')}{dt'}\right]_g \approx \frac{e\cos\theta}{m}\exp\left(-t'\Gamma\cos\theta\right)\frac{F_0\tau\sqrt{\pi}}{1.17} \times \exp\left\{-\frac{\tau^2\left(\omega_0^2 - \Gamma^2\cos^2\theta\right)}{5.4756}\right\} \times \cos\left\{\phi + \frac{k\omega_0^2\tau^2\cos\theta}{2.7378}\right\}.$$

https://doi.org/10.1017/S0263034610000741 Published online by Cambridge University Press

For Lorentzian pulse:

$$\left[\frac{d\delta_y(t')}{dt'}\right]_l \approx \frac{e\cos\theta}{m}\exp\left(-t'\Gamma\cos\theta\right)\frac{F_0\tau\pi}{1.29}\cos(\phi) \times \exp\left\{-\frac{\tau\left(\omega_0^2+\Gamma^2\cos^2\theta\right)^{1/2}}{1.29}\right\}.$$

For hyperbolic secant pulse:

$$\left[\frac{d\delta_y(t')}{dt'}\right]_h \approx \frac{e\cos\theta}{m}\exp\left(-t'\Gamma\cos\theta\right)\frac{F_0\tau\pi}{3.52} \times \left[e^{i\phi}\sec h\left\{\frac{\tau\pi}{3.52}(\omega_0 - i\Gamma\cos\theta)\right\} + e^{-i\phi}\sec h\left\{-\frac{\tau\pi}{3.52}(\omega_0 + i\Gamma\cos\theta)\right\}\right]$$

Substituting these values of $\left(d\delta_y(t')/dt'\right)$ in Eq. (1), we find that the decay time of the reflected field $f_1(t')$ is $t_0 \sim 1/\Gamma\cos(\theta)$. For proper choice of the plasma density, angle of incidence, thickness of the plasma layer, t_0 can be much larger than the period of the main pulse. This field embodies the reflected main few-cycle pulse along with the left over field, which persists after the passage of the main pulse. This Wakefield is quasistatic and its magnitude depends on CEP, angle of incidence, plasma layer parameters, pulse-shape, and number of cycles in the laser pulse. An analytic expression for the frozen-in Wakefield has been derived by Varró (2007) in the approximation in which the duration of the Wakefield has been assumed to be infinite. However, in this approximation, the specific effect of pulse-shape is smeared out. In order to include the effect of pulse-shape on the reflected field, we solve the equation of motion exactly by employing the fifth order Runge-Kutta method. We find that the magnitude of the quasistatic frozen-in electric field (Wakefield) is about 10^{-3}–10^{-4} of the main pulse. The numerical results are shown in Figures 1, 2, and 3.

3. DEPENDENCE OF HIGH HARMONIC GENERATION ON THE PULSE-SHAPE OF AN ULTRASHORT, INTENSE, FEW CYCLE LASER IN THE REFLECTED RADIATION FROM A THIN, DENSE PLASMA LAYER

In the interaction of obliquely incident, ultrashort, ultraintense, few-cycle laser with a thin plasma layer, surface current is generated. The equation of motion of the electron in the plasma is given by $d\vec{p}/dt = e\left(\vec{E} + \vec{v}/c \times \vec{B}\right)$, and $d\left(m\gamma c\right)/dt = e/c\left(\vec{v}.\vec{E}\right)$ where $\vec{p} = m\gamma\vec{v}$, $\vec{E}$, and $\vec{B}$ are electric and magnetic field vector associated with the laser light, $\vec{v} = d\vec{\delta}/dt$ is the local velocity of the electron, and γ is the relativistic factor given by $\gamma = 1/\sqrt{\left(1 - v^2/c^2\right)}$. Solving equation of motion of the electron for the component of displacement vector perpendicular and parallel to $\vec{k}$ denoted by $\delta_\perp$ and δ_{II} respectively, one obtains:

$$\frac{d\delta_\perp}{d\xi} = \frac{e}{m}\exp\left(-\xi\Gamma\cos\theta\right)\int_{-\infty}^{\xi} F(\xi)\exp\left(\xi\Gamma\cos\theta\right)d\xi \qquad (3)$$

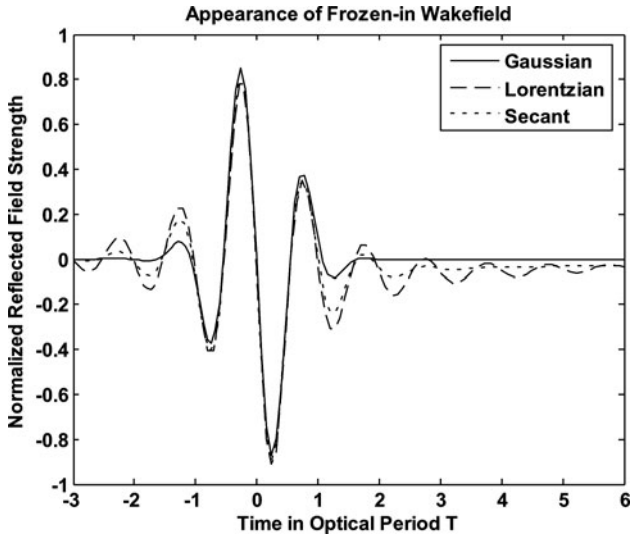

Fig. 1. Shows the appearance of frozen-in Wakefield originating from a single cycle incident laser pulse having different pulse-shape. The angle of incidence in each case is 56 degree, and CE phase = 0. Bold line represents the magnitude of the field from the laser pulse with Gaussian, dashed line for Lorentzian, and the dotted line for hyperbolic secant pulse-shape. The thickness of metal layer is 2 mm, $\lambda = 800$ nm, center carrier frequency $\omega_0 = 2.36 \times 10^{15}\text{s}^{-1}$, free electron density is 10^{22} cm^{-3} and the electric field strength of the reflected signal is normalized by $F_0/35$ (F_0 is the peak value of the incoming laser field).

and

$$\frac{d\delta_{II}}{d\xi} = \frac{1}{2c}\left[\left(\frac{d\delta_\perp}{d\xi}\right)^2\right]. \qquad (4)$$

where $\xi = t' - \delta_{II}/c$ is exact retarded time at the position of the electrons. The y-component of local velocity $d\delta_y/d\xi$ can be

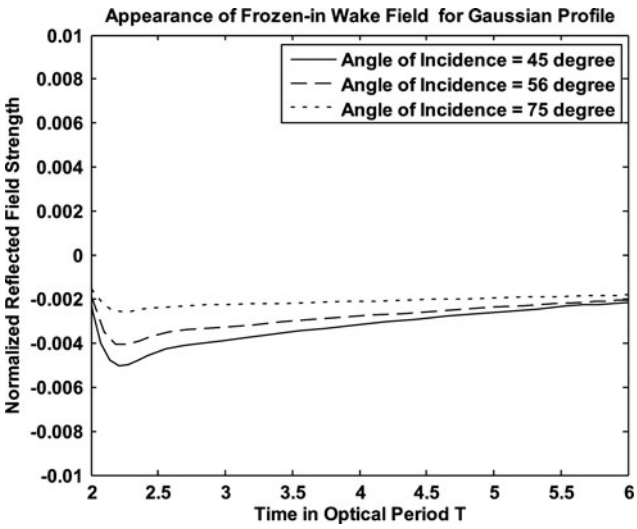

Fig. 2. Represents the variation of the frozen-in Wakefields reflected field strength as a function of normalized retarded time with angles of incidence as parameter corresponding to the incident Gaussian pulse-shape. The CE phase has been chosen to be zero. The thickness of metal layer is 2 mm, free electron density is 10^{22} cm^{-3}, $\lambda = 800$ nm, $l = 2$ nm, center carrier frequency $\omega_0 = 2.36 \times 10^{15}\text{s}^{-1}$, and the electric field strength of the reflected signal is normalized by $F_0/35$.

https://doi.org/10.1017/S0263034610000741 Published online by Cambridge University Press

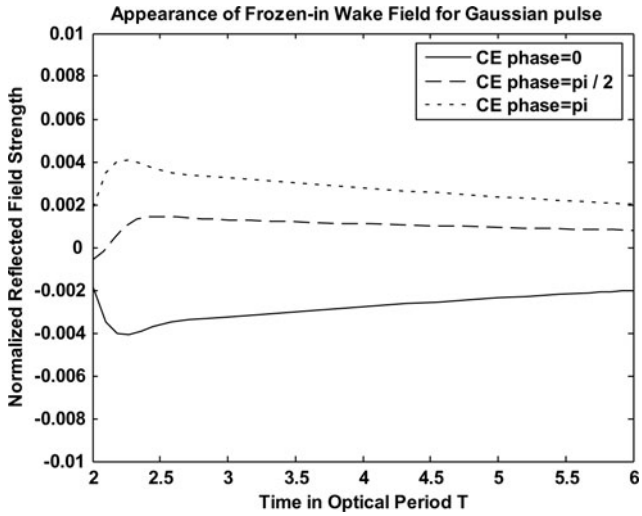

Fig. 3. Shows the variation of the Wakefields as a function of normalized retarded time with CE phase as parameter corresponding to the incident Gaussian pulse-shape. The angle of incidence has been chosen to be 56 degree, $l = 2$ mm, free electron density is 10^{22} cm^{-3}, $\lambda = 800$ nm, center carrier frequency $\omega_0 = 2.36 \times 10^{15}$s^{-1}, and the electric field strength of the reflected signal is normalized by $F_0/35$.

expressed in terms of $d\delta_\perp/d\xi$:

$$\frac{d\delta_y}{d\xi} = \frac{d\delta_\perp}{d\xi}\cos\theta + \frac{1}{2c}\left(\frac{d\delta_\perp}{d\xi}\right)^2 \sin\theta. \tag{5}$$

Fourier transforms of f_1 (ξ) yields the reflected field in frequency domain:

$$f_1(\omega) = -\frac{m\Gamma}{e}\frac{d\delta_y(\omega)}{dt'} = -\frac{m\Gamma}{e}\int_{-\infty}^{\infty}\left(\frac{d\delta_y}{d\xi}\right)\exp\left[i\omega\left(\xi + \frac{\delta_{II}(\xi)}{c}\right)\right]d\xi. \tag{6}$$

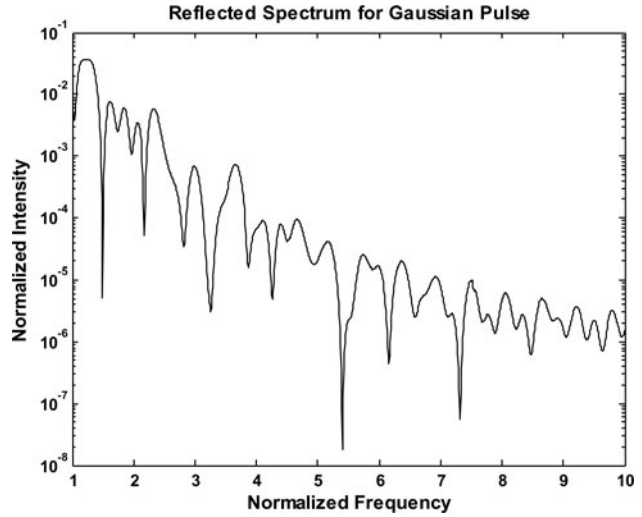

Fig. 4. Depicts the variation of the normalized harmonic intensity with normalized frequency ω/ω_0, when the incident few-cycle ($p = 2$) pulse is Gaussian. The chosen parameters are: CE phase = 0, number of cycles in a pulse are $p = 2$, free electron density 10^{21} cm^{-3}, intensity of incident laser light = 4×10^{18} W/cm^2, angle of incidence = 70 degree, $\lambda = 800$ nm, center carrier frequency $\omega_0 = 2.36 \times 10^{15}$s^{-1}, and the thickness of metal layer $l = 8$ nm.

The Fourier transform of local velocity for the Lorentz pulse-shape can be obtained as (Appendix):

$$\begin{aligned}\frac{d\delta_y(\omega)}{dt'} \approx \exp\left(\frac{i\beta^2\omega\tau\pi}{5.16}\right)\times\int_{-\infty}^{\infty} d\xi L(\xi) \\ \times\exp\left[i\omega\xi\left(1+\frac{\beta^2}{2\left\{1+\left(\frac{1.29\xi}{\tau}\right)^2\right\}}\right)\right] \\ \times\exp\left[i\omega\beta^2\frac{\tau}{2.58}\tan^{-1}\left(\frac{1.29\xi}{\tau}\right)\right],\end{aligned} \tag{7}$$

where

$$\begin{aligned}\frac{L(\xi)}{c} = \sum_n J_n\left(\frac{\beta^2\omega}{2\omega_0\left\{1+\left(\frac{1.29\xi}{\tau}\right)^2\right\}^2}\right) \\ \times\left[\frac{-i\beta\cos\theta}{\left\{1+\left(\frac{1.29\xi}{\tau}\right)^2\right\}}\left\{e^{iA(1-2n)} - e^{iA(1+2n)}\right\}\right. \\ \left. + \frac{\beta^2\sin\theta}{2\left\{1+\left(\frac{1.29\xi}{\tau}\right)^2\right\}^2}\left\{\begin{matrix}2e^{-i2nA} - e^{-i2A(1-n)} \\ -e^{-2iA(1+n)}\end{matrix}\right\}\right]\end{aligned} \tag{8}$$

The value of the Fourier transform of local velocity for the hyperbolic secant pulse-shape is given by (Appendix):

$$\begin{aligned}\frac{d\delta_y(\omega)}{dt'} \approx \exp\left(-\frac{i\beta^2\omega\tau}{1.76}\right)\times\int_{-\infty}^{\infty} d\xi\, H(\xi)\exp[i\omega\xi] \\ \times\exp\left[i\omega\beta^2\frac{\tau}{1.76}\tanh\left(\frac{1.76\xi}{\tau}\right)\right],\end{aligned} \tag{9}$$

where

$$\begin{aligned}\frac{H(\xi)}{c} = \sum_n J_n\left[\beta^2\frac{\omega}{2\omega_0}\left\{\sec h\left(\frac{1.76\xi}{\tau}\right)\right\}^2\right] \\ \times\left[-i\beta\sec h\left(\frac{1.76\xi}{\tau}\right)\cos\theta\left\{e^{iA(1-2n)} - e^{iA(1+2n)}\right\}\right. \\ \left. + \frac{\beta^2}{2}\left\{\sec h\left(\frac{1.76\xi}{\tau}\right)\right\}^2\sin\theta\left\{2e^{-i2nA} - e^{-i2A(1-n)} - e^{-2iA(1+n)}\right\}\right].\end{aligned} \tag{10}$$

The value of the Fourier transform of local velocity the Gaussian pulse-shape can be expressed as (Appendix):

$$\begin{aligned}\frac{d\delta_y(\omega)}{dt'} \approx \int_{-\infty}^{-p} G(\xi)\times\exp(i\omega\xi)d\xi + \int_{-p}^{+p} G(\xi)\times\exp\left\{i\omega\xi(1+\beta^2)\right\} \\ \times\exp(i\beta^2 p\omega)d\xi + \int_{p}^{\infty} G(\xi)\times\exp(i\omega\xi)\times\exp(2i\beta^2 p\omega)d\xi,\end{aligned} \tag{11}$$

https://doi.org/10.1017/S0263034610000741 Published online by Cambridge University Press

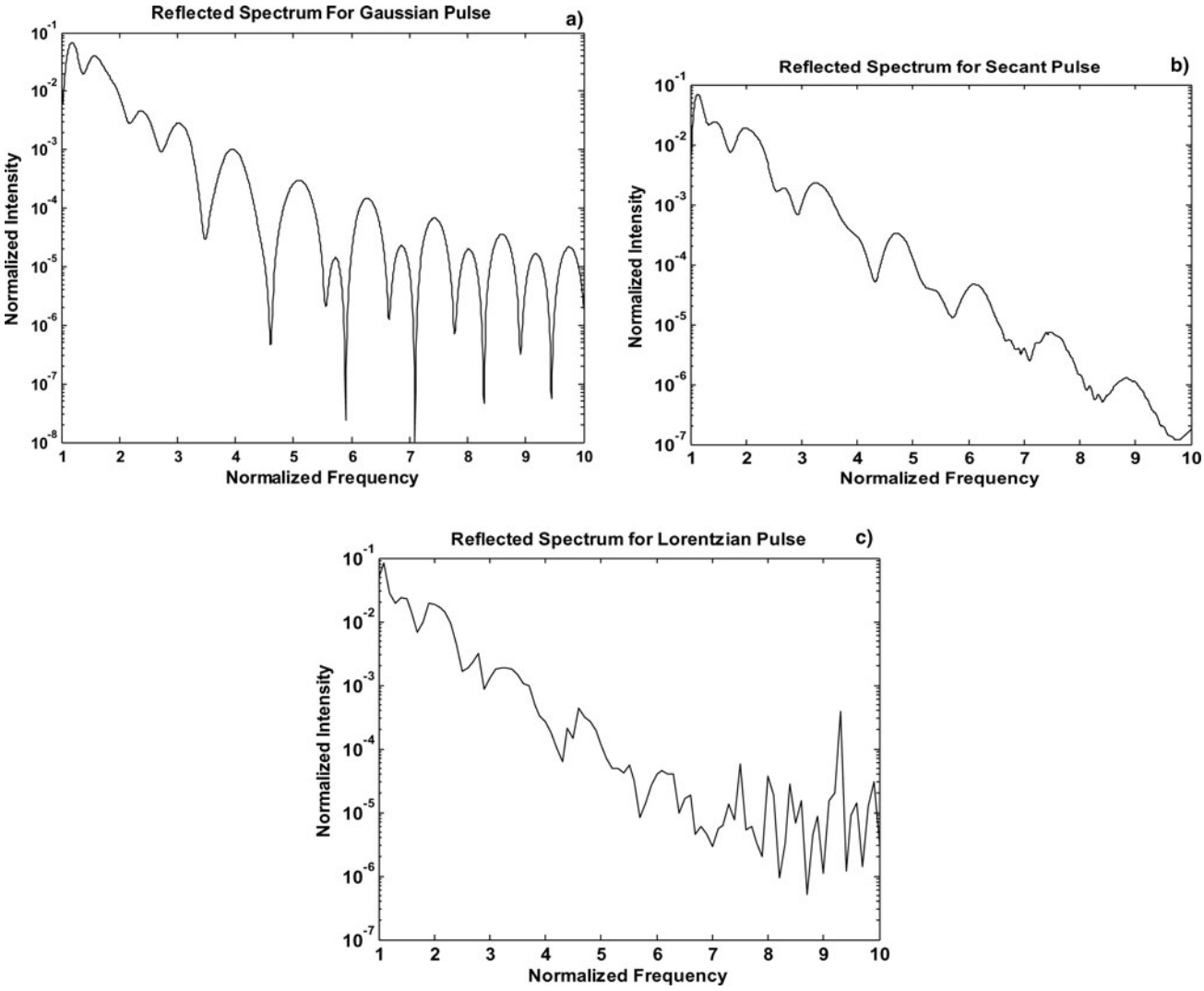

Fig. 5. (**a**) represents the generation of high harmonics in reflected spectrum for single cycle ($p = 1$) Gaussian pulse. The chosen parameters are: CE phase = 0, free electron density 10^{22} cm^{-3}, intensity of incident laser light = 4×10^{18} W/cm^2, angle of incidence = 45 degree, $\lambda = 800$nm, $\omega_0 = 2.36 \times 10^{15}$s^{-1}, and $l = 8$ nm. (**b**) represents the generation of high harmonics in reflected spectrum for single cycle ($p = 1$) hyperbolic secant pulse. The chosen parameters are: CE phase = 0, free electron density 10^{22} cm^{-3}, intensity of incident laser light = 4×10^{18} W/cm^2, angle of incidence = 45 degree, $\lambda = 800$nm, $\omega_0 = 2.36 \times 10^{15}$s^{-1}, and $l = 8$ nm. (**c**) represents the generation of high harmonics in reflected spectrum for single cycle ($p = 1$) Lorentzian pulse. The chosen parameters are: CE phase = 0, free electron density 10^{22} cm^{-3}, intensity of incident laser light = 4×10^{18} W/cm^2, angle of incidence = 45 degree, $\lambda = 800$nm, $\omega_0 = 2.36 \times 10^{15}$s^{-1}, and $l = 8$ nm.

where $p = \frac{\tau\sqrt{\pi}}{2.34\sqrt{2}}$, and

$$\frac{G(\xi)}{c} = \sum_n J_n \left[\beta^2 \frac{\omega}{2\omega_0} \exp\left\{ -2\left(\frac{1.17\xi}{\tau}\right)^2 \right\} \right] \times \left[-i\beta\cos\theta \left\{ e^{iA(1-2n)} - e^{iA(1+2n)} \right\} \exp\left\{ -\left(\frac{1.17\xi}{\tau}\right)^2 \right\} + \frac{\beta^2}{2} \sin\theta \left\{ 2e^{-i2nA} - e^{-i2A(1-n)} - e^{-2iA(1+n)} \right\} \times \exp\left\{ -2\left(\frac{1.17\xi}{\tau}\right)^2 \right\} \right]. \quad (12)$$

4. RESULTS AND DISCUSSION

We present our results when an intense few-cycle, ultrashort laser pulse interacts with a preformed highly inhomogeneous over-dense thin (thickness of the film $l \ll \lambda$) plasma layer. Numerical results show that there remains a quasistatic left over field. The duration of the existence of the quasistatic Wakefield depends on the optimum choice of the plasma density, thickness of the plasma layer, and angle of incidence. The magnitude and sign of the Wakefield are found to depend on the pulse-shape, number of cycles in the pulse, and CEP. Figure 1 shows the appearance of frozen-in Wakefields caused by single cycle incident laser pulse having Gaussian, Lorentzian, and hyperbolic secant pulse-

https://doi.org/10.1017/S0263034610000741 Published online by Cambridge University Press

shape. The relative magnitudes of the Wakefields due to Gaussian, Lorentzian, hyperbolic secant pulse are found to be in the ratio 1:14:12. An explanation for different magnitudes of the fields created can be given in terms of the duration for which the different pulses last. It is noted that the tail of the Lorentzian pulse goes to zero at a slower rate than the other two. Gaussian pulse decreases to zero at the fastest rate. All these pulses have single cycle, and same FWHM. When such pulses are incident on thin plasma layer then pulse front sweeps this surface creating a superluminal polarization wave described by the local displacement. The laser pulse profiles, which have larger interaction time and are in phase with electron motion, can transfer more energy to the electron. Such a coherent motion is responsible for frozen-in Wakefields of varying magnitudes. Figure 2 represents the variation of the frozen-in Wakefields with the retarded time (t'/T) for angles of incidence (θ) corresponding to Gaussian pulse. It is found that with increasing θ, the magnitude of frozen-in Wakefield decreases. This is because, when a single cycle, ultrashort p-polarized TM-laser pulse, is obliquely incident on plasma layer then the y-component of the electric field E_y is responsible for frozen in Wakefields. This field is which is proportional to cos θ. Figure 3 depicts the variation of the Wakefield with time (t'/T) keeping the carrier-envelope (CE) phase constant, corresponding to Gaussian pulse. The effects of CE phase are dominant only in the case of laser pulses whose duration is definitely less than about 10 optical cycles. The amplitude and sign of these Wakefields can be modulated by changing the CE phase of the incoming pulse.

The reflected radiation also exhibits the presence of high harmonics of the incident laser pulse. Figure 4 represents the variation of the normalized harmonic intensity with normalized frequency ω/ω_0, when the incident few-cycle ($p =$ 2) pulses are Gaussian. Figures 5.1, 5.2, 5.3 show the generation of high harmonics in reflected spectrum for single cycle ($p = 1$) pulse corresponding to Gaussian, hyperbolic secant, and Lorentzian pulses respectively. Figure 6 shows the variation of the normalized intensity of the harmonics in the reflected radiation caused by the incident secant laser pulse. Maximum intensity is found at $\omega = 2\omega_0$. Higher harmonics are found with decreasing intensities. Figure 7 depicts the effect of the variation of the CE phase on the intensity of the reflected harmonic at $\omega = 2\omega_0$ caused by a single cycle Gaussian pulse. Figure 8 represents the variation of the

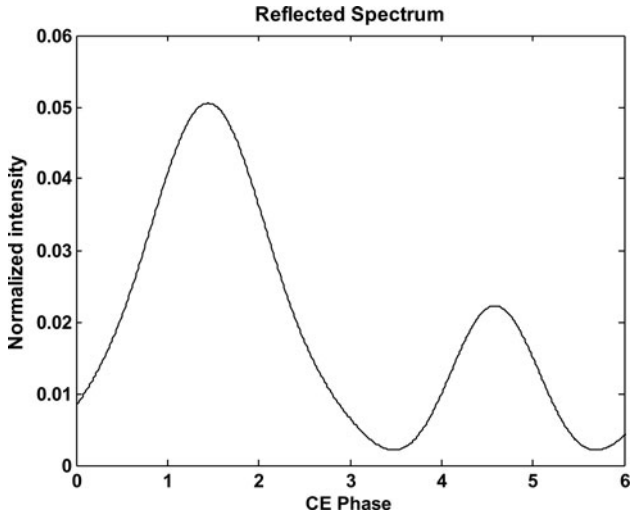

Fig. 7. Depicts the effect of variation of the CE phase on the intensity of the reflected harmonic at $\omega = 2\omega_0$ caused by a single cycle Gaussian pulse. The results shown are for free electron density $10^{22}\,\mathrm{cm}^{-3}$, intensity of incident laser light $= 4 \times 10^{18}$ W/cm^2, angle of incidence = 45 degree, $\lambda = 800$nm, $\omega_0 = 2.36 \times 10^{15}\mathrm{s}^{-1}$, and $l = 8$ nm.

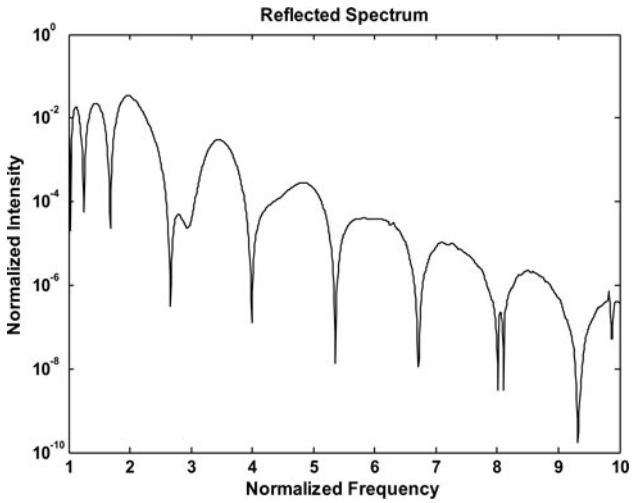

Fig. 6. Shows the variation of the normalized intensity of the harmonics in the reflected radiation caused by the incident single cycle hyperbolic secant laser pulse. The parameters are; CE phase = 1.5 radian, free electron density $10^{22}\,\mathrm{cm}^{-3}$, intensity of incident laser light $= 4 \times 10^{18}$ W/cm^2, angle of incidence = 50 degree, $\lambda = 800$nm, $\omega_0 = 2.36 \times 10^{15}\mathrm{s}^{-1}$ and $l = 8$ nm.

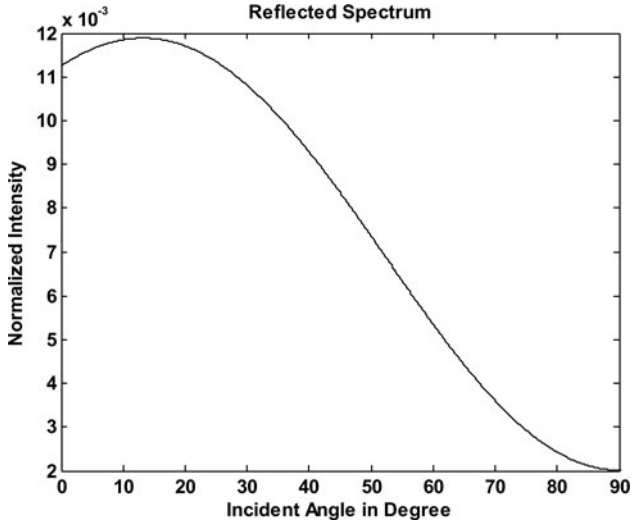

Fig. 8. Shows the variation of the intensity of the $2\omega_0$ harmonic with angle of incidence corresponding to the incident single cycle Gaussian pulse. Numerical results are for free electron density $10^{22}\,\mathrm{cm}^{-3}$, intensity of incident laser light $= 4 \times 10^{18}$ W/cm^2, CE phase = 0 radian, $\lambda = 800$nm, $\omega_0 = 2.36 \times 10^{15}\mathrm{s}^{-1}$, and $l = 8$ nm.

https://doi.org/10.1017/S0263034610000741 Published online by Cambridge University Press

intensity of the $2\omega_0$ harmonic with angle of incidence caused by a single cycle Gaussian pulse.

5. CONCLUSION

In conclusion, this paper presents an analytical and numerical investigation of the interaction of the different laser-pulse-envelope shape with a thin plasma layer, which gives rise to HHG and Wakefield generation. Our numerical results show that the reflected radiation exhibits the presence of quasi-static "frozen-in" Wakefield in the time-domain and high harmonics of the incident laser pulse in frequency domain. The harmonic peaks are found to depend upon carrier-envelope phase difference, number of cycles, angle of incidence, and thickness of the plasma layer. The magnitude of the Wakefield is also found to depend on CEP, and angle of incidence. The Wakefield decays in a time which varies inversely to the product of the squared plasma frequency and thickness of plasma layer.

ACKNOWLEDGMENTS

Financial support from the Department of Science & Technology, New-Delhi (Government of India) is thankfully acknowledged. The authors are very-much thankful to the Referees for their valuable suggestions. The authors are thankful to Professor Naresh Dadhich, Vice-Chancellor, V. M. O. U. Kota for support, encouragement, and his keen interest in the outcome of this work. Authors are thankful to Professor N. K. Jaiman, Head, Department of Pure and Applied Physics, University of Kota, Kota for several academic discussions, support, and encouragement. Authors are thankful to Mr. Rakesh Sharma, and Professor M. K. Ghadoliya for administrative support.

REFERENCES

Baeva, T., Gordienko, S. & Pukhov, A. (2006). Theory of high-order harmonic generation in relativistic laser interaction with overdense plasma. *Phys. Rev. E* **74**, 046404–1/046404-11.

Bingham, R., Mendonça, J.T. & Shukla, P.K. (2004). Plasma based charged-particle accelerators. *Plasma Phys. Contr. Fusion* **46**, R1–R23.

Brabec, T. & Krausz, F. (1997). Nonlinear optical pulse propagation in the single-cycle regime. *Phys. Rev. Lett*. **78**, 3282–3285.

Brabec, T. & Krausz, F. (2000). Intense few-cycle laser fields: Frontiers of nonlinear optics. *Rev. Mod. Phys*. **72**, 545–591.

Brügge, D.A. & Pukhov, A. (2007). Propagation of relativistic surface harmonics radiation in free space. *Phys. Plasmas* **14**, 093104–11.

Bulanov, S.S., Macchi, A., Maksimchuk, A., Matsuoka, T., Nees, J. & Pegoraro, F. (2007). Electromagnetic pulse reflection at self-generated plasma mirrors: laser pulse shaping and high order harmonic generation. *Phys. plasmas* **14**, 093105–093105.10.

Bulanov, S.V., Esirkepov, T.ZH., Naumova, N.M. & Sokolov, I.V. (2003). Relativistic whistle: high order harmonics induced by the ultra-intense laser pulse propagating inside the fiber. *Phys. Rev. E*. **67**, 016405–10.

Dromey, B., Kar, S., Bellei, C., Carroll, D.C., Clarke, R.J., Green, J.S., Kneip, S., Markey, K., Nagel, S.R., Simpson, P.T., Willingale, L., McKenna, P., Neely, D., Najmudin, Z., Krushelnick, K., Norreys, P.A. & Zepf, M. (2007). Bright multi-KeV harmonic generation from relativistically oscillating plasma surfaces. *Phys. Rev. Lett*. **99**, 0850011–14.

Dromey, B., Rykovanov, S.G., Adams, D., Hörlein, R., Nomura, Y., Carroll, D.C., Foster, P.S., Kar, S., Markey, K., McKenna, P., Neely, D., Geissler, M., Tsakiris, G.D. & Zepf, M. (2009). Tunable enhancement of high harmonic emission from laser solid interactions. *Phys. Rev. Lett*. **102**, 225002–4.

Foldes, I.B., Kocsis, G., Racz, E., Szatmari, S. & Veres, G. (2003). Generation of high harmonics in laser plasmas. *Laser Part. Beams* **21**, 517–521.

Ganeev, R.A. (2009). Generation of high-order harmonics of high-power lasers in plasmas produced under irradiations of solid target surfaces by a pre-pulse. *Phys.-Uspekhi* **52**, 55–77.

Gupta, M.K., Sharma, R.P. & Mahmoud, S.T. (2007). Generation of plasma wave and third harmonic generation at ultra relativistic laser power. *Laser Part. Beams* **25**, 211–218.

Kieffer, J.C., Matte, J.P., Pépin, H., Chaker, M., Beaudoin, Y., Johnston, T.W., Chien, C.Y., Coe, S., Mourou, G. & Dubau, J. (1992). Electron distribution anisotropy in laser-produced plasmas from x-ray line polarization measurements. *Phys. Rev. Lett*. **68**, 480–483.

Linde, D.V. (1999). Generation of high order optical harmonics from solid surfaces. *Appl. phys. B* **68**, 315–319.

Malka, V., Fritzler, S., Lefebvre, E., Aleonard, M.M., Burgy, F., Chambaret, J.P., Chemin, J.F., Krushelnick, K., Malka, G., Mangles, S.P.D., Najmudin, Z., Pittman, M., Rousseau, J.P., Scheurer, J.N., Walton, B. & Dangor, A.E. (2002). Electron acceleration by a wake field forced by an intense ultrashort laser pulse. *Sci*. **298**, 1596–1600.

Nisoli, M., Sansone, G., Stagira, S., Silvestri, S.D., Vozzi, C., Pascolini, M., Poletto, L., Villoresi, P. & Tondello, G. (2003). Effects of carrier-envelope phase differences of few optical-cycle light pulses in single-shot high- order-harmonic spectra. *Phys. Rev. Lett*. **91**, 2139051–54.

Norreys, P.A., Santala, M., Clark, E., Zepf, M., Watts, I., Beg, F.N., Krushelnick, K., Tatarakis, M., Dangor, A.E., Fang, X., Graham, P., McCanny, T., Singhal, R.P., Ledingham, K.W.D., Creswell, A., Sanderson, D.C.W., Magill, J., Machacek, A., Wark, J.S., Allott, R., Kennedy, B. & Neely, D. (1999). Observation of a highly directional γ-ray beam from ultrashort, ultraintense laser pulse interactions with solids. *Phys. Plasmas* **6**, 2150–2157.

Nuzzo, S., Zarcone, M., Ferrante, G. & Basile, S. (2000). A simple model of high harmonic generation in a plasma. *Laser Part. Beams* **18**, 483–487.

Quéré, F., Thaury, C., Geindre, J.P., Bonnaud, G., Monot, P. & Martin, Ph. (2008). Phase properties of laser high-order harmonics generated on plasma mirrors. *Phys. Rev. Lett*. **100**, 0950041–0950044.

Quéré, F., Thaury, C., Monot, P., Dobosz, S. & Martin, Ph. (2006). Coherent wake emission of high order harmonics from overdense plasmas. *Phys. Rev. Lett*. **96**, 1250041–1250044.

Sprangle, P. (1987). Analysis of radiation focusing and steering in the free-electron laser by use of a source-dependent expansion technique. *Phys. Rev. A* **36**, 2773–2781.

Varró, S. (2007). Linear and nonlinear absolute phase effects in interactions of ultrashort laser pulses with a metal nano-layer or with a thin plasma layer. *Laser Part. Beams* **25**, 379–390.

Villoresi, P., Barbiero, P., Poletto, L., Nisoli, M., Cerullo, G., Priori, E., Stagira, S., Lisco, C. De, Bruzzese, R. & Altucci, C. (2001). Study of few-optical-cycles generation of high-order harmonics. *Laser Part. Beams* **19**, 41–45.

Vshivkov, V.A., Naumova, N.M., Pegoraro, F. & Bulanov, S.V. (1998). Nonlinear electrodynamics of the interaction of ultra-intense laser pulses with a thin foil. *Phys. Plasmas* **5**, 2727–2741.

Zepf, M., Clark, E.L., Beg, F.N., Clarke, R.J., Dangor, A.E., Gopal, A., Krushelnick, K., Norreys, P.A., Tatarakis, M., Wagner, U. & Wei, M.S. (2003). Proton acceleration from high intensity laser interactions with thin foil targets. *Phys. Rev. Lett.* **90**, 064801–4.

APPENDIX

Derivation of Fourier Transform of Local Velocity for Lorentz Pulse-Shape

Using Eq. (3) the value of the derivative $d\delta_\perp/d\xi$ for the Lorentz pulse-shape can be obtained approximately as:

$$\frac{d\delta_\perp}{d\xi} \approx \frac{eF_0}{m\omega_0} \times \frac{\sin(\omega_0\xi + \phi + \alpha)}{\left[1 + \left(\frac{1.29\xi}{\tau}\right)^2\right]\sqrt{1 + \left(\frac{\Gamma\cos\theta}{\omega_0}\right)^2}}, \tag{13}$$

where

$$\alpha = \sin^{-1}\left[\frac{\frac{\Gamma\cos\theta}{\omega_0}}{\sqrt{1 + \left(\frac{\Gamma\cos\theta}{\omega_0}\right)^2}}\right]. \tag{14}$$

Substituting Eq. (13) in Eq. (4) and integrating, we obtain:

$$\frac{\delta_{II}}{c} \approx 2\beta^2\left[\frac{\tau}{10.32}\left\{\pi + 2\tan^{-1}\left(\frac{1.29\xi}{\tau}\right) + \frac{2.58\xi}{\tau\left[1 + \left(\frac{1.29\xi}{\tau}\right)^2\right]}\right\} - \frac{\sin(2A)}{4\omega_0\left[1 + \left(\frac{1.29\xi}{\tau}\right)^2\right]^2}\right], \tag{15}$$

where $A = \omega_0\xi + \phi + \alpha$, and

$$\beta = \frac{eF_0}{2mc\omega_0} \times \frac{1}{\sqrt{1 + \left(\frac{\Gamma\cos\theta}{\omega_0}\right)^2}}. \tag{16}$$

Also, using Eq. (5) and Eq. (13), we get:

$$\frac{1}{c}\frac{d\delta_y}{dt} \approx \frac{2\beta\sin(A)\cos\theta}{\left[1 + \left(\frac{1.29\xi}{\tau}\right)^2\right]} + \frac{2\beta^2\sin^2(A)\sin\theta}{\left[1 + \left(\frac{1.29\xi}{\tau}\right)^2\right]^2}. \tag{17}$$

Fourier transforming Eq. (17), we get

$$\frac{d\delta_y(\omega)}{dt'} \approx \exp\left(\frac{i\beta^2\omega\tau\pi}{5.16}\right) \times \int_{-\infty}^{\infty} d\xi\, L(\xi) \times \exp\left[i\omega\xi\left(1 + \frac{\beta^2}{2\left\{1 + \left(\frac{1.29\xi}{\tau}\right)^2\right\}}\right)\right] \times \exp\left[i\omega\beta^2\frac{\tau}{2.58}\tan^{-1}\left(\frac{1.29\xi}{\tau}\right)\right], \tag{18}$$

where

$$\frac{L(\xi)}{c} = \left[\frac{2\beta\sin(A)\cos\theta}{\left\{1 + \left(\frac{1.29\xi}{\tau}\right)^2\right\}} + \frac{2\beta^2\sin^2(A)\sin\theta}{\left\{1 + \left(\frac{1.29\xi}{\tau}\right)^2\right\}^2}\right] \times \exp\left(-\frac{i\omega\beta^2\sin(2A)}{2\omega_0\left\{1 + \left(\frac{1.29\xi}{\tau}\right)^2\right\}^2}\right). \tag{19}$$

Making use of the well known Bessel identity $e^{-iz\sin(\theta)} = \sum_n J_n(z)e^{-in\theta}$, Eq. (19) gives:

$$\frac{L(\xi)}{c} = \left[\frac{2\beta\sin(A)\cos\theta}{\left\{1 + \left(\frac{1.29\xi}{\tau}\right)^2\right\}} + \frac{2\beta^2\sin^2(A)\sin\theta}{\left\{1 + \left(\frac{1.29\xi}{\tau}\right)^2\right\}^2}\right] \times \sum_n J_n\left(\frac{\beta^2\omega}{2\omega_0\left[1 + \left(\frac{1.29\xi}{\tau}\right)^2\right]^2}\right) \times \exp(-2inA)$$

$$\Rightarrow \frac{L(\xi)}{c} = \sum_n J_n\left(\frac{\beta^2\omega}{2\omega_0\left\{1 + \left(\frac{1.29\xi}{\tau}\right)^2\right\}^2}\right) \times \left[\frac{-i\beta\cos\theta}{\left\{1 + \left(\frac{1.29\xi}{\tau}\right)^2\right\}}\left\{e^{iA(1-2n)} - e^{iA(1+2n)}\right\} + \frac{\beta^2\sin\theta}{2\left\{1 + \left(\frac{1.29\xi}{\tau}\right)^2\right\}^2} \times \left\{2e^{-i2nA} - e^{-i2A(1-n)} - e^{-2iA(1+n)}\right\}\right]. \tag{20}$$

https://doi.org/10.1017/S0263034610000741 Published online by Cambridge University Press

Derivation of Fourier Transform of Local Velocity for Hyperbolic Secant Pulse-Shape

Using Eq. (3) the value of the derivative $d\delta_\perp/d\xi$ for the hyperbolic secant pulse-shape can be obtained approximately as:

$$\frac{d\delta_\perp}{d\xi} \approx \frac{eF_0}{m\omega_0} \times \sec h\left(\frac{1.76\xi}{\tau}\right) \times \frac{\sin\left(\omega_0\xi + \phi + \alpha\right)}{\sqrt{1 + \left(\frac{\Gamma\cos\theta}{\omega_0}\right)^2}}. \tag{21}$$

Substituting Eq. (21) in Eq. (4) and then integrating we obtain:

$$\frac{\delta_{II}}{c} \approx 2\beta^2\left[\frac{\tau}{3.52}\left\{\tanh\left(\frac{1.76\xi}{\tau}\right) - 1\right\} - \frac{\left\{\sec h\left(\frac{1.76\xi}{\tau}\right)\right\}^2 \sin(2A)}{4\omega_0}\right]. \tag{22}$$

Substituting Eq. (21) in Eq. (5) one obtains:

$$\frac{1}{c}\frac{d\delta_y}{d\xi} \approx 2\beta\left\{\sec h\left(\frac{1.76\xi}{\tau}\right)\right\}\sin(A)\cos\theta + 2\left\{\sec h\left(\frac{1.76\xi}{\tau}\right)\right\}^2 \beta^2 \sin^2(A)\sin\theta \tag{23}$$

Fourier transforming Eq. (23), we get

$$\frac{d\delta_y(\omega)}{dt'} \approx \exp\left(-\frac{i\beta^2\omega\tau}{1.76}\right) \times \int_{-\infty}^{\infty} d\xi\, H(\xi)\exp[i\omega\xi] \times \exp\left[i\omega\beta^2\frac{\tau}{1.76}\tanh\left(\frac{1.76\xi}{\tau}\right)\right], \tag{24}$$

where

$$\frac{H(\xi)}{c} = \left[2\beta\sec h\left(\frac{1.76\xi}{\tau}\right)\sin(A)\cos\theta + 2\left\{\sec h\left(\frac{1.76\xi}{\tau}\right)\right\}^2\beta^2\sin^2(A)\sin\theta\right] \times \exp\left[-i\frac{\omega^2}{2\omega_0\beta}\left\{\sec h\left(\frac{1.76\xi}{\tau}\right)\right\}^2\sin(2A)\right]. \tag{25}$$

Further using Bessel identity, Eq. (25) gives:

$$\begin{aligned}\frac{H(\xi)}{c} &= \left[2\beta\sec h\left(\frac{1.76\xi}{\tau}\right)\sin(A)\cos\theta + 2\left\{\sec h\left(\frac{1.76\xi}{\tau}\right)\right\}^2\beta^2\sin^2(A)\sin\theta\right] \times \sum_n J_n\left[\beta^2\frac{\omega}{2\omega_0}\left\{\sec h\left(\frac{1.76\xi}{\tau}\right)\right\}^2\right] \times \exp(-2inA),\\ \Rightarrow \frac{H(\xi)}{c} &= \sum_n J_n\left[\beta^2\frac{\omega}{2\omega_0}\left\{\sec h\left(\frac{1.76\xi}{\tau}\right)\right\}^2\right] \times \left[-i\beta\sec h\left(\frac{1.76\xi}{\tau}\right)\cos\theta \times \left\{e^{iA(1-2n)} - e^{iA(1+2n)}\right\} + \frac{\beta^2}{2}\left\{\sec h\left(\frac{1.76\xi}{\tau}\right)\right\}^2\sin\theta \times \left\{2e^{-i2nA} - e^{-i2A(1-n)} - e^{-2iA(1+n)}\right\}\right].\end{aligned}$$

Derivation of Fourier Transform of Local Velocity for Gaussian Pulse-Shape

Using Eq. (3) the value of the derivative $d\delta_\perp/d\xi$ for the Gaussian pulse-shape can be obtained approximately as:

$$\frac{d\delta_\perp}{d\xi} \approx \frac{eF_0}{m\omega_0} \times \exp\left\{-\left(\frac{1.17\xi}{\tau}\right)^2\right\} \times \frac{\sin\left(\omega_0\xi + \phi + \alpha\right)}{\sqrt{1 + \left(\frac{\Gamma\cos\theta}{\omega_0}\right)^2}}. \tag{26}$$

Substituting Eq. (26) in Eq. (5) one obtains:

$$\frac{1}{c}\frac{d\delta_y}{d\xi} \approx 2\beta\left\{\exp\left\{-\left(\frac{1.17\xi}{\tau}\right)^2\right\}\right\}\sin(A)\cos\theta + 2\left\{\exp\left\{-\left(\frac{1.17\xi}{\tau}\right)^2\right\}\right\}^2\beta^2\sin^2(A)\sin\theta \tag{27}$$

Fourier transforming, we get

$$\begin{aligned}\frac{d\delta_y(\omega)}{dt'} \approx{}& \int_{-\infty}^{-p} G(\xi)\times\exp(i\omega\xi)d\xi + \int_{-p}^{+p} G(\xi)\times\exp\left\{i\omega\xi\left(1+\beta^2\right)\right\} \times \exp\left(i\beta^2 p\omega\right)d\xi + \int_{p}^{\infty} G(\xi)\times\exp(i\omega\xi)\times\exp\left(2i\beta^2 p\omega\right)d\xi,\end{aligned} \tag{28}$$

https://doi.org/10.1017/S0263034610000741 Published online by Cambridge University Press

where $p = \tau\sqrt{\pi}/2.34\sqrt{2}$, and

$$\frac{G(\xi)}{c} = \left[2\beta \sin(A)\cos\theta \exp\left\{-\left(\frac{1.17\xi}{\tau}\right)^2\right\} + 2\beta^2 \sin^2(A)\sin\theta \exp\left\{-2\left(\frac{1.17\xi}{\tau}\right)^2\right\}\right] \times \exp\left[-i\frac{\omega}{2\omega_0}\exp\left\{-2\left(\frac{1.17\xi}{\tau}\right)^2\right\}\beta^2 \sin(2A)\right]. \quad (29)$$

Using the Bessel identity, Eq. (29) gives:

$$\frac{G(\xi)}{c} = \sum_n J_n\left[\beta^2\frac{\omega}{2\omega_0}\exp\left\{-2\left(\frac{1.17\xi}{\tau}\right)^2\right\}\right] \times \left[-i\beta\cos\theta\left\{e^{iA(1-2n)} - e^{iA(1+2n)}\right\}.\times \exp\left\{-\left(\frac{1.17\xi}{\tau}\right)^2\right\} + \frac{\beta^2}{2}\sin\theta\left\{2e^{-i2nA} - e^{-i2A(1-n)} - e^{-2iA(1+n)}\right\} \times \exp\left\{-2\left(\frac{1.17\xi}{\tau}\right)^2\right\}\right].$$

https://doi.org/10.1017/S0263034610000741 Published online by Cambridge University Press